AGU100 ADVANCING EARTH AND SPACE SCIENCE

Tectonics

RESEARCH ARTICLE
10.1029/2018TC005053

Special Section:
The 2016 Central Italy Seismic Sequence: Insights, implications and lessons learned

Tectonics Inversions, Fault Segmentation, and Triggering Mechanisms in the Central Apennines Normal Fault System: Insights From High-Resolution Velocity Models

M. Buttinelli[1], **G. Pezzo**[1], **L. Valoroso**[1], **P. De Gori**[1], **and C. Chiarabba**[1]

[1]Istituto Nazionale di Geofisica e Vulcanologia, Rome, Italy

Abstract The potential role of subsequent tectonic phases in reworking inherited geological structures is a key issue to unravel the seismotectonics of an area. This has a direct connection with fault segmentation, earthquakes maximum magnitude, and strong implications for seismic hazard assessment. The central Apennines (Italy) represent an exemplary case, since it developed because of the overprint of different deformational phases, producing potential conditions for episodic tectonic inversions and a very complex structural architecture. In this paper, we show how inherited compressional structures, still dominating the Apennines belt architecture, interfere with the active extension, having a direct connection with active seismotectonics. We present seismicity and new velocity tomograms of an 80-km-long section of the normal fault system activated during the 2009 and 2016–2018 seismic sequences. The joint interpretation highlights how the extensional seismic sequences partially reactivated inherited compressive structures, which have not an undisputable relationship with the surficial geological setting. Complexity deriving from the irregular geometry of normal faults and inverted thrust ramps is responsible for the observed intense fragmentation of the extensional system. Fluid overpressure seems to be a viable mechanism behind the partial remobilization of unbroken segments of the fault system.

Key Points:
- Tectonic inversions and fault segmentations represent the main process behind the current crustal arrangement of central Apennines
- Surface versus deep expression of faults: subsequent deformational stages cause complex interaction between inherited extensional and compressional structures
- Fluid overpressure plays a role in the partial remobilization of unbroken fault segments

Correspondence to:
M. Buttinelli,
mauro.buttinelli@ingv.it

Citation:
Buttinelli, M., Pezzo, G., Valoroso, L., De Gori, P., & Chiarabba, C. (2018). Tectonics inversions, fault segmentation, and triggering mechanisms in the central Apennines normal fault system: Insights from high-resolution velocity models. *Tectonics*, *37*. https://doi.org/10.1029/2018TC005053

Received 12 MAR 2018
Accepted 16 OCT 2018
Accepted article online 18 OCT 2018

1. Introduction

Broad mountain belts characterized by diffuse deformation and seismicity suggest that continental deformation is a complex process related to strong lateral variations of lithosphere structure and its rheology (Brace & Kohlstedt, 1980; Cloetingh & Burov, 1996; Jackson, 1995; Ranalli & Murphy, 1987; Ziegler et al., 1995). In this wide context, the preexisting faults and shear zones may act as main long-living lithospheric weaknesses during the orogen development, also favoring reactivation episodes and tectonic inversions (Pfiffner, 2017, and references therein).

The reactivation of inherited structures has deep implications both during compressional and extensional phases (e.g., Coward, 1994; Jackson, 1980). Indeed, the fault irregular geometry, the favorable or unfavorable orientation within the active stress regime, and the fault length play an important role on the fault segmentation and maximum magnitude of individual earthquakes (e.g., Cowie et al., 2012; Martínez-Garzón et al., 2015). Focusing on the Mediterranean orogens, clear examples of positive inversions are widely documented where large normal faults of the tethysian margin were reactivated during the thrust-and-fold belt formation (Butler et al., 2004; Butler & Mazzoli, 2006; Coward, 1994; Mazzoli et al., 2000).

In this context, the continuous recycling of preexisting structures is potentially common also for the Apennines, since episodes of extension and compression alternated in space and time during the Tethys evolution first, and in the more recent Apennines mountain chain building (Di Domenica et al., 2012; Scisciani, 2009).

Previous episodes of large-scale extensional faults developed during the Permo-Triassic incipient stages of Tethys ocean formation along the Adria continental margins (e.g., Calamita et al., 2003, and references therein). Even if their existence has been widely invoked in order to explain the surficial architecture of peculiar sedimentary successions pointing to the existence of structural highs and lows, the distribution of those structures and their orientation is still poorly constrained. A second set of extensional faults have been associated to the Miocene bending of the Adria paleo margin foreland domain before the Apennines

compression (Bigi et al., 2011; Scisciani et al., 2014). The general migration of the coupled pair of extension and compression during Apennines buildup phase often led areas previously deformed in compression to be the site of extension, and vice versa (e.g., Barchi et al., 1998).

Seismological observations show that past decades normal faulting earthquakes interfere with the preexisting thrust-related structures (Chiarabba & Amato, 2003). Such process enhances the fault segmentations and complexities during the rupture evolution, like those observed in the recent large earthquakes of the Apennines (Cheloni et al., 2017; Chiaraluce et al., 2017; Pizzi et al., 2017; Scognamiglio et al., 2018; Tinti et al., 2016).

Multiple mainshock sequences are common expression of the Apennines tectonics and widely documented by historical (Rovida et al., 2011) and recent seismicity (Chiarabba et al., 2015). The enduring energy release pattern testifies for a complex interaction between adjacent faults and triggering phenomena, which include static and dynamic stress transfer between faults (Freed, 2005) and pore fluid pressure migration (Chiarabba et al., 2009; Di Luccio et al., 2010; Malagnini et al., 2012).

During the past decades, several $M > 5.5$ normal faulting earthquakes ruptured contiguous portions of the NW trending central Apennines extensional system (Figure 1a), basically segmented at a kilometer scale, such as the *Mw*6.1 2009 L'Aquila (Chiarabba et al., 2009; Valoroso et al., 2013) and the *Mw*6.1 to *Mw*6.5 2016 Amatrice (Tinti et al., 2016), and Norcia earthquakes (Scognamiglio et al., 2018). The normal faulting systems are set on top of a delaminating Adria lithosphere (Carannante et al., 2013; Chiarabba & Chiodini, 2013; Chiarabba et al., 2005), which provides the mechanism to the downwarping of the Adria crust and the uplift and tilting of the thrust units accreted to the mountain range (Figure 1b).

The aim of this study is to provide an original view of normal faulting mechanisms in the Apennines, trying to address how structural complexities influence the interaction between adjacent faults and triggering processes, giving also elements that might be useful for short-term hazard scenarios.

We show the present-day architecture of the normal faulting system by combining high-resolution velocity models with high-quality earthquake locations (Valoroso et al., 2013) from the 2009 normal faulting L'Aquila earthquake sequences. We focus on the Monti della Laga-Gorzano fault (MLGf) as a prominent unbroken segment of the 150-km-long system, which was partially interested by the 2009 and the 2016–2017 seismic sequences.

2. Geologic Outline

During the Neogene evolution of the Apennines, compression of the Adria continental margin generated large-scale noncylindrical thrust-and-fold structures, mainly involving Meso-Cenozoic sedimentary sequences (Bally et al., 1986; Centamore et al., 1993; Castellarin et al., 1978; Centamore et al., 1993). The deep structure of the central Apennines, as well as the deformation styles (thick- vs. thin-skinned tectonics), is still debated within the scientific community (Barchi et al., 1998; Butler et al., 2004; Pfiffner, 2017; Scrocca et al., 2003).

Following the thin-skinned view, compression progressively migrated eastward, with generation of in-sequence sets of relatively shallow low dipping thrusts (Doglioni, 1991; Patacca et al., 1990; Scrocca et al., 2007). On the other hand, the thick-skinned models imply the involvement of the basement with preexisting extensional faults of the tethysian continental margin partially inverted and rotated (Calamita et al., 2003; Di Domenica et al., 2012; Scisciani et al., 2014). Although the debate is still vivid, some authors (e.g., Calabrò et al., 2003; Scrocca et al., 2005; Shiner et al., 2004; Tozer et al., 2002) proposed mixed models comprehending subsequent thin- and thick-skinned tectonic styles for the central and southern Apennines.

During Late Pliocene and Quaternary, widespread extension propagated through the belt, with the development of several intrachain basins and crustal-scale normal faults (Mazzoli et al., 2000). Currently active extension develops on NW trending fault systems that run along the mountain range dislocating the compressional edifice (Figure 1). While surface topography is still mimicking the thrust-related deep-rooted folds, intramountain basins mark the activity of range-bounding normal faults (Bosi et al., 2003; Palumbo et al., 2004; Pucci et al., 2014). Large earthquakes of the last three decades ruptured 10- to 25-km-long contiguous fault segments reaching an about 150-km-long section of the belt (Figure 1a). However, one fault segment remained particularly silent, that is, a NNW trending lineament at the base of

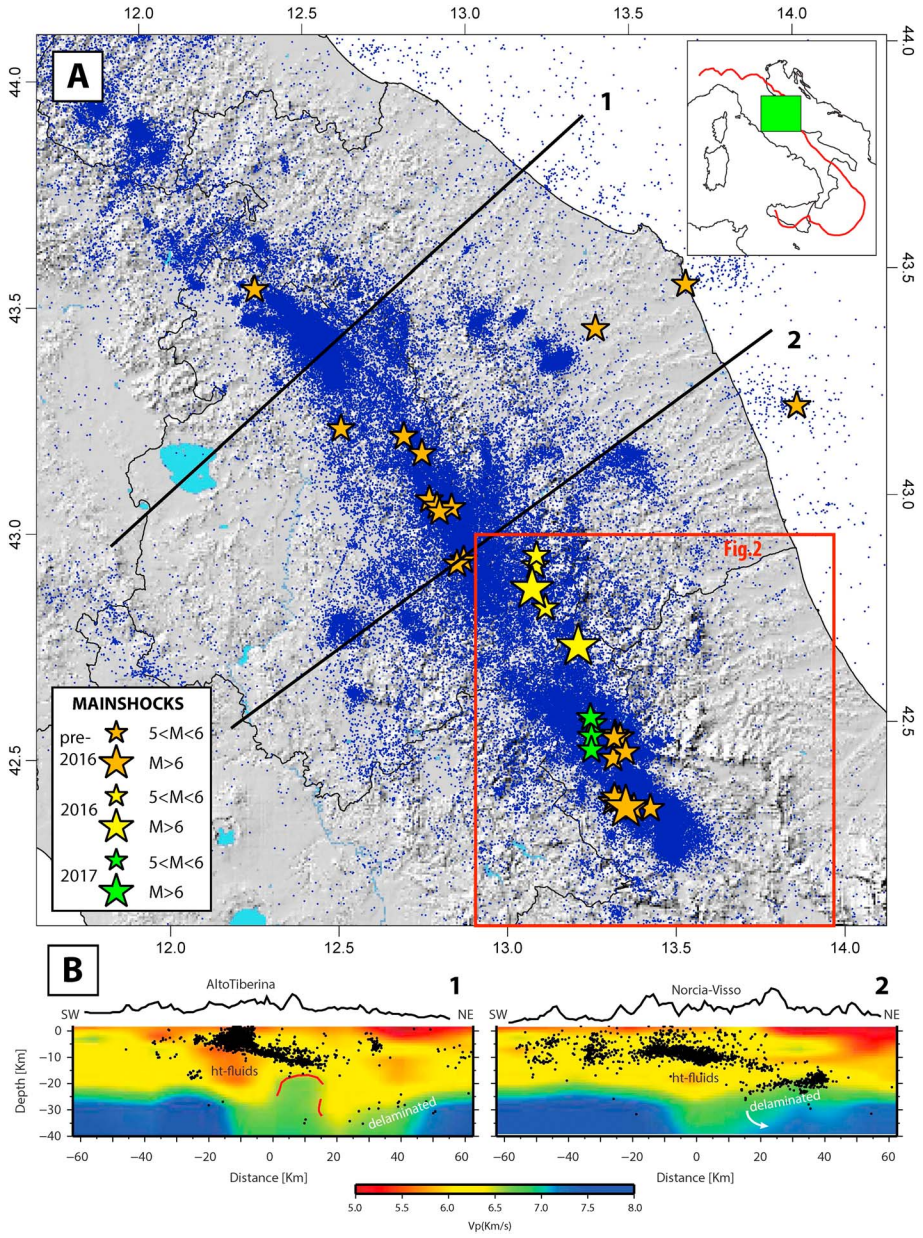

Figure 1. (a) Seismicity of past decades in central Apennines (modified from Chiarabba et al., 2015). Large-magnitude events are shown. (b) Seismicity distribution and velocity images along two transects crossing the central Apennines (modified from Carannante et al., 2013) describing large-scale tectonic processes currently affecting the orogeny.

the Laga mountain range called MLGf (Galadini & Galli, 2003). Although Bigi et al. (2011) estimated a maximum cumulative offset of about 1,000 m for this fault, a detailed timing of fault activity remains uncertain. Its surface expression and activity and the connection with deep structures and relationship with the seismicity have been discussed and questioned in the recent literature (Bigi et al., 2013, 2011; Improta et al., 2012). The MLGf encompasses the northern segment of the 2009 L'Aquila seismic sequence (i.e., Campotosto segment in Valoroso et al., 2013) and the southern termination of the normal fault system activated on August 2016 during the 2016–2017 central Italy one. In particular, on January 2017 this area experienced four $M_W > 5$ earthquakes (green stars in Figure 1). Although Bigi et al. (2013) deeply discussed about the surface expression of the fault and the deep segment along which the 2009 seismicity developed, other authors, based on geological and paleoseismological data, pose evidences that $Mw > 6.5$ earthquakes can develop on this fault (Galadini & Galli, 2003).

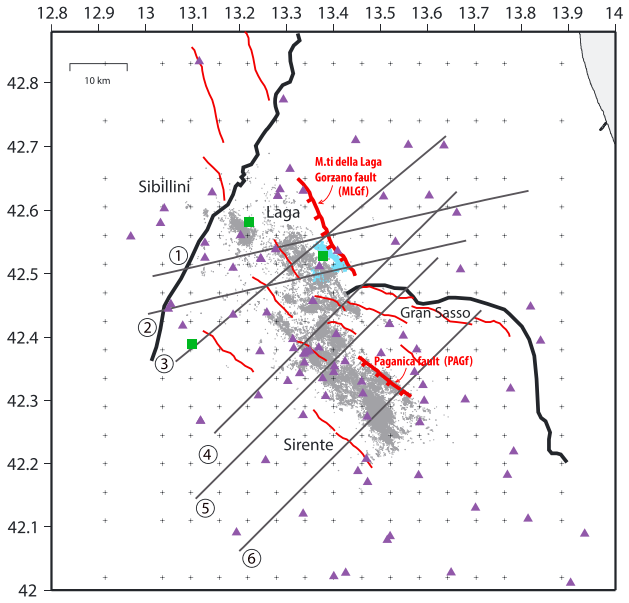

Figure 2. Tomographic inversion model setup: grid nodes (crosses) and seismic stations (triangles). The 2009 seismicity from Valoroso et al. (2013; gray dots). Normal faults traces (red lines) and principal thrust superficial traces (Sibillini and Gran Sasso systems, black solid lines) are reported (after Centamore et al., 1992; Di Domenica et al., 2012; Valoroso et al., 2013. Deep wells locations (green squares) and traces of vertical velocity profiles shown in Figure 4.

3. Earthquake Catalog and Tomographic Models

During the 2009 L'Aquila earthquake sequence, a huge amount of seismologicalt data was recorded by a dense temporary network (Chiaraluce et al., 2011; Margheriti et al., 2011) and processed to extract one of the top data sets for normal faulting earthquakes (Valoroso et al., 2013). In order to compute tomographic models, we use data recorded at up to 108 permanent and temporary stations, relative to about 2,000 $M_L > 2.5$ aftershocks recorded in the first 3 months of the seismic sequence. The high-quality data set extends the model resolution to an area wider than that previously obtained with a smaller number of data by Di Stefano et al. (2011). Our new model improves the resolution of the one proposed by Carannante et al. (2013; 15 × 15 × 4 km) for the overlapping area. We inverted a total of 59,044 *P* waves and 29,833 *S* wave arrivals to resolve a 5 × 5-km horizontal grid of nodes with vertical layers spaced every 2 km (Figure 2). A final root-mean-square of 0.10 s with a variance improvement of 57% was reached after four iteration steps, using the linearized, iterative, damped least squares inversion method Simulps-14q (Eberhart-Phillips & Reyners, 1997, and references therein) to simultaneously determine three-dimensional V_p and V_p/V_s models and earthquake locations.

To assess model resolution and reliability, the full resolution matrix (Toomey & Foulger, 1989) has been analyzed, selecting the value of spread function (spf) that encompasses the well-resolved volumes of the V_p and V_p/V_s models. Visually inspecting the averaging vectors (Toomey & Foulger, 1989), we select a very conservative value of the spf threshold for well-resolved parameters (1.5), much smaller than the value indicative of good resolution by the analysis (spf = 2.0, white line in Figure 3).

Tomographic models show *P* wave velocity and V_p/V_s continuously varying within the target volume. Geological discontinuities like faults appear in tomograms as velocity gradients rather than sharp velocity changes. Thus, their tentative interpretation is principally constrained by the general shape of velocity anomalies. Positive compressional structures appear as relatively large length V_p anomalies in tomograms (Figure 4), averaging over smaller-scale details like imbricated or thrust stack systems that cannot be individually imaged. Conversely, the extensional structures are mostly represented by negative and relatively more squared V_p anomalies. In this study, we anchored the interpretation with independent data available from seismic profiles and deep wells (see Bigi et al., 2013, 2011; Mariucci & Montone, 2016; Porreca et al., 2018). According to *P* wave velocity for the lithologies of the area (Bally et al., 1986; Barchi et al., 1998; Latorre et al., 2016), we associate V_p = 5.5–6.5 km/s to carbonate and dolomite rocks and V_p = 3.5–4 km/s to Laga turbidites. The V_p range between 4.0 and 5.5 km/s can be associated to the Umbria-Marche Succession, mostly made of alternations of shallow-to-deep calcareous and clayey units. These values are also in agreement with broad-scale geologic reconstructions (Bigi et al., 2011; Scisciani & Montelfalcone, 2005). This correspondence is verifiable for most of the resolved volume, as we observe through the consistence between the tomograms velocity distribution around the Varoni-1 well area and the well velocity distribution (section 1 in Figure 4). Anyway, the velocity of the topmost layer in some regions (i.e., the Gran Sasso range) cannot be fully resolved for the lack of data coverage.

We focus on the relationship between the crustal structure and seismicity, comparing the new high-resolution V_p and V_p/V_s models with the high-precision aftershock catalog of Valoroso et al. (2013). It consists of relative relocations for more than 60k events, characterized by a M_L0.7 completeness magnitude and by a location accuracy on the order of tens to hundreds of meters.

4. Deep Structure and Geometry of the Normal Fault System

During the 2009 sequence, earthquakes originated in the topmost 10 km of the crust on two en echelon SW dipping and NW trending fault segments, corresponding to the surface expression of the Paganica fault

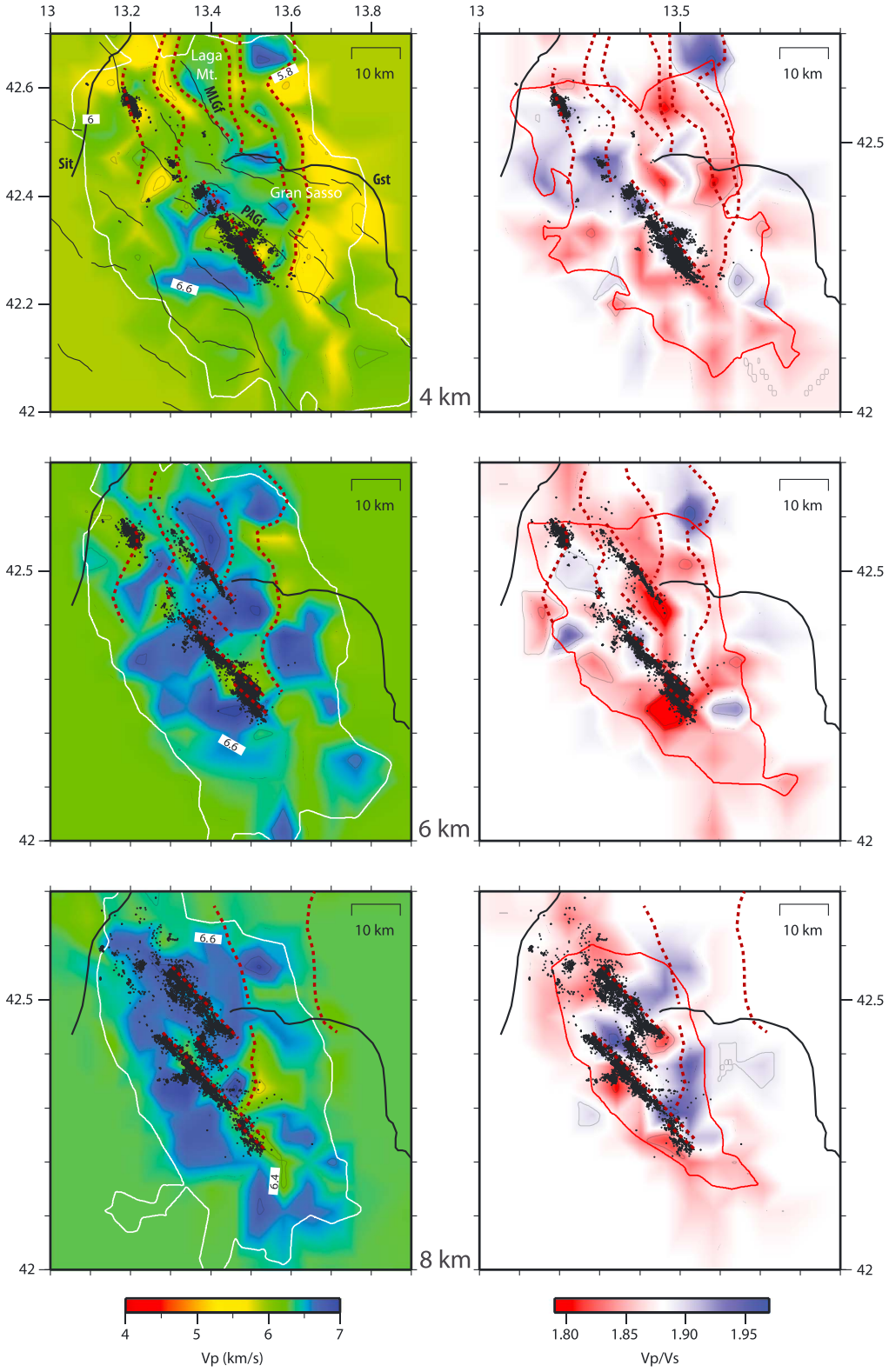

Figure 3. Map velocity distribution at 4-, 6-, and 8-km depths for V_p (left panels) and V_p/V_s (right panels). Seismicity occurred at ±1 km from each layer is plotted (after Valoroso et al., 2013). Velocity contour lines at 0.2 km/s for V_p and 0.02 for V_p/V_s. The well-resolved volume is defined by spread functions (white solid line for V_p and red solid line for V_p/V_s) enclosing 70% of the diagonal elements (see also Eberhart-Phillips & Reyners, 1997). Black solid lines represent the surface expression of main extensional faults. Dotted lines represent main buried thrusts lineaments interpreted by tomography.

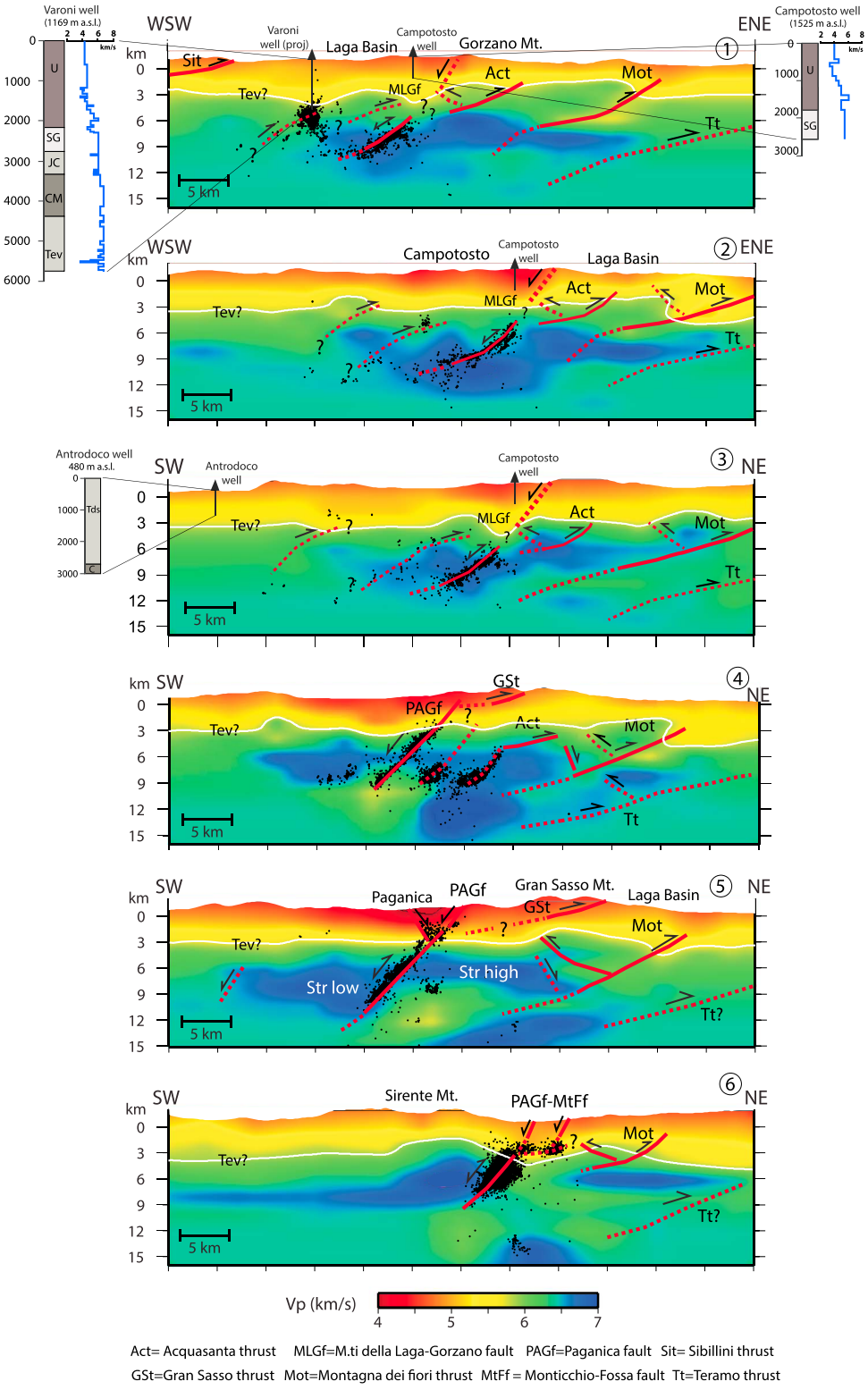

Figure 4. Vertical sections of V_p model across the MLGf (1–3) and PAGf (4–6 traces in Figure 2). The stratigraphy of the deep wells is used to constrain the interpretation. White lines refer to the top of the Triassic evaporates (TEv). Aftershocks from Valoroso et al. (2013) are shown as black dots. The main faults, drawn jointly interpreting tomograms and seismicity, are represented by solid (highly constrained) and dashed (more inferred) red lines. Downhole velocities available for Varoni-1 and Campotosto-1 wells are reported after Mariucci and Montone (2016). MLGf = Monti della Laga-Gorzano fault; PAGf = Paganica fault.

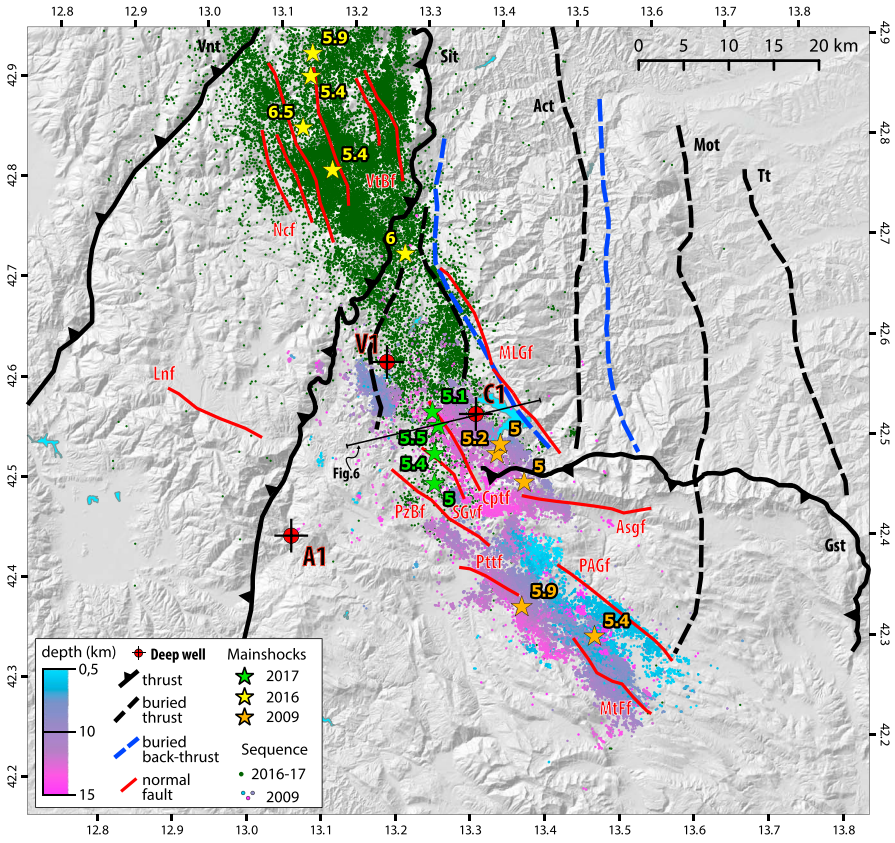

Figure 5. Synthetic map of the area showing the principal structural elements. Solid black are thrusts: Sit (Sibillini), Vnt (Val Nerina), Gst (Gran Sasso); solid red are normal faults: MLGf (Monti della Laga-Gorzano), Asgf (Assergi), Cptf (Capitignano), SGvf (San Giovanni), PzBf (Pizzoli-Barete), Pttf (Pettino), VtBf (Mt.Vettore-Bove system), Ncf = Norcia system, Lnf (Leonessa), PAGf (Paganica), MtFf (Monticchio-Fossa). Dashed lines represent buried thrusts and back thrusts: Act (Acquasanta), Mot (Mon-tagna dei fiori), Tt (Teramo), after Bigi et al. (2013) and consistent with the interpretation of velocity tomograms in Figure 4. Larger earthquakes that occurred in 2009 and 2016–2017 are shown as stars. The 2009 aftershocks are represented by cyan-to-pink dots (Valoroso et al., 2013), while green dots (without a color code for the lower resolution of hypocentral depths) are for 2016–2017 aftershocks sequence (Chiaraluce et al., 2017). Deep wells are shown (A1 = Antrodoco 1, V1 = Varoni 1, C1 = Campotosto 1).

(PAGf, Figure 3*)* and northward spreading to the MLGf. Velocity pattern shows that the overall geometry of the upper crust is still dominated by compressive features (Figure 3). The high resolution allows retrieving the geometry of geological structures even at a scale of few kilometers, much smaller than that obtained by previous works (e.g., Carannante et al., 2013). Between 4- and 8-km depths, N-S trending thrusts dislocate the Mesozoic carbonate multilayer and the basement, up to the Gran Sasso Mountain range (Figure 3). These compressive structures bound the expression of the MLGf and PAGf segments confining the seismicity distribution.

4.1. The MLGf Segment

The geological evidences of the MLGf segment have been investigated by previous works (Bigi et al., 2013; Boncio, Lavecchia, Milana, & Rozzi, 2004; Boncio, Lavecchia, & Pace, 2004; Falcucci et al., 2018; Galadini & Galli, 2003; Lavecchia et al., 2016). This fault segment was also the site of several moderate-magnitude earthquakes ($Mw < 5.5$) during the 2009 and 2016–2018 seismic sequences (see Figure 5). Earthquakes aligned on an about 15-km-long NNW trending fault, confined between 5- and 10-km depths (see also Valoroso et al., 2013). The closeness to the Campotosto artificial lake dam (the second artificial water reservoir in Europe for extension) represents a main issue that requires a full understanding of seismic potential of the area, also in reason of the increased public concern and seismic hazard perception during the last seismic sequence.

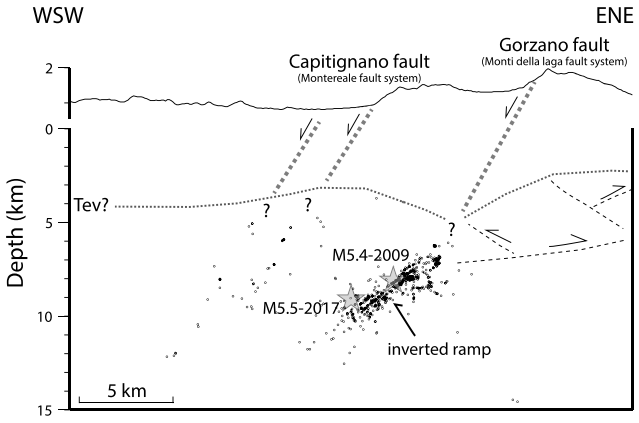

Figure 6. Zoom on the Monti della Laga-Gorzano fault segment, showing the main structural elements (trace line in Figure 5). Note that the seismicity occurred in 2009 (black dots) and the largest earthquakes of 2009 and 2017 (stars) are located on the deep ramp, below 5-km-depth. Dotted line (Tev) represents the top of the Triassic evaporites also interpreted in Figure 4. Thick dashed lines represent the interpolation of main fault traces from surficial data. Thin dashed lines represent main shallow thrusts interpreted in Figure 4.

Velocity anomalies across the area (Figure 4) reveal three main thrust systems, in accordance with the geological interpretation of seismic profiles (Bigi et al., 2011). Those structures are traceable down to 9-km depth suggesting the involvement of the basement (Figure 4). The three systems consist of main east verging thrusts with associated west verging back thrusts. From east to west the deeper and more external is the Teramo thrust (Tt); an intermediate one forming the Montagna dei Fiori (Mot) and the shallower one forming the Acquasanta (Act) anticline. A more internal structure is resolved to the west of the Gorzano Mountain, entirely buried beneath the Laga basin (Figure 4, section 1), defined by a bumped velocity pattern between 3- and 6-km depths. Since the high V_p body (top of the blue body in section 1) is shallower in the fault footwall, we hypothesize that this can be representative of a large-scale normal fault bordering a Mesozoic structural high. Velocity warping and bumping in the hanging wall also indicate a not complete positive inversion of the fault during the compressional phase (Figure 4, sections 1 to 3). We interpret this inverted segment as one of the first compressive structures of the area, subsequently affected by compression on the more external systems.

Following this reconstruction, the Gorzano Mountain is the expression of the paired system of NS trending thrust and back thrust (Act) that are responsible for the uplift of the antiform (Figures 4 and 5). Part of the dislocation observable at the surface, largely associated to the activity of the MLGf, can be then addressed to this compressional phase.

The 2009 seismicity developed in fact along the Act deep ramp, suggesting a further ongoing negative inversion of the ramp (sections 1–3 in Figure 4). Intriguingly, seismicity is confined between 5 and 10 km of depth, while no events are located at shallow depths (between 0 and 5 km), despite the very low completeness magnitude (M_L0.7) of the 2009 aftershock catalog. This might suggest a lack of vertical continuity between deep and shallow portion of the MLGf. We remark that the upper termination of the deep ramp potentially coincides with the upper tip of the back thrust that originally uplifted the Gorzano structure (Figure 6). In this view, the January 2017 larger-magnitude earthquakes (green stars in Figure 5) occurred at the northwestern termination of the MLGf fault activated in 2009. The recent large earthquakes developed on the same deep ramp activated in 2009, with hypocenters mostly located at the lower tip of the previous seismicity (Figure 6). The updip prolongation of the deep ramp matches with the MLGf superficial expression, but we cannot address further either the continuity of the fault or the shallow detachment, as suggested by Bigi et al. (2013).

4.2. The PAGf Segment

This segment ruptured during the 2009 M_W6.1 mainshock that propagated for about 16 km along strike (Cirella et al., 2012). The progressive transition from the Monti della Laga to the Gran Sasso structures is unraveled by the velocity models in sections 3 to 5 (Figure 4). The external Tt, Mot, and Act thrust systems continue southward plunging below the Gran Sasso mountain range. Prolonged activity of these thrusts was responsible for the current topography, with uplift and tilt of the entire structure in agreement with the Cardello and Doglioni (2015) model.

Here the positive tectonic inversion seems to play a minor role with respect to the northern areas. In fact, the velocity anomaly associated to the PAGf preserves the original extensional features (Figure 4, section 5). To the east, SW dipping faults are rooted within the high V_p basement. In this central area (Figure 4, section 4), seismicity and velocity pattern suggest the existence of preserved extensional highs and lows of the Mesozoic carbonate multilayer and basement, of which the PAGf is the principal feature.

At the southern termination of the segment (Figure 4, sections 5 and 6), seismicity spreads at the border of a high V_p anomaly centered beneath the Sirente Mountain range. In this section, the Mesozoic normal fault has been inverted during the thrusting episode. Aftershocks spread over a large volume around the inverted ramp and along the shallow subhorizontal flat portion of the thrust. Underneath the Gran Sasso range, the southern continuation of the NS thrust (Mot) is still visible at the southern termination of the PAGf segment.

5. Discussion

Earthquakes interaction and remobilization of relict faults represent a challenging issue for the accurate assessment of seismic hazard. Fault interaction may lead to multiple mainshock sequences as frequently observed worldwide (e.g., Fletcher et al., 2016; Hamling et al., 2017; Sieh et al., 1993).

In the Apennines, multiple shocks came along with repeated tectonic changes that likely create the conditions for fault inversion. The currently active extensional belt (D'Agostino et al., 2009; Serpelloni et al., 2005) spreads on the mountain range, whose architecture derives from repeated episodes of compression (e.g., Bigi et al., 2011; Cardello & Doglioni, 2015; Scisciani et al., 2014).

Velocity tomograms and refined hypocenter locations show deformation on a variety of fault segments and strands whose degree of complexity agrees with that observed by field geology (see also Valoroso et al., 2014). We observe V_p patterns (warping and bumping of velocity anomalies), which might be interpreted as evidence for flat and ramp thrust systems that originated during compression by recycling preexisting normal faults bordering Mesozoic structural highs (Figure 4) and connected to shallow low angle flats. During the Apennines compression, the propagation of thrusts interfered and was limited by high-velocity heterogeneities of the basement presumably generated during the Mesozoic rifting of the continental lithosphere, conditioning the lateral extent and the propagation of faults.

In the present-day extension, the lateral extent of normal faults outlined by aftershock distribution is limited by the NS trending thrusts (Figure 5), that causes a first-order segmentation of the normal faulting belt (see also Chiarabba & Amato, 2003). Repeated and doubled inversion of preexisting structures during the former compression and the current extension induced a fragmentation of the belt.

North of the Gran Sasso Range, mainly N-S thrust ramps currently slip as extensional faults (Scisciani et al., 2014). Those structures apparently continue for several kilometers beneath the thin-skinned structures of the Gran Sasso range (see tomograms of Figure 4 and Mot of Figure 5), as also proposed by Cardello and Doglioni (2015), which is in contrast with the low-shortening model proposed by Scisciani et al. (2014). Conversely, in the surroundings of PAGf, the active normal faults are generally trending NW-SE, reactivate previous thrust ramps, which in turn reactivated Mesozoic inherited normal faults with more clear evidences. One interesting point of discussion (which is not the direct focus of this work) is if those faults at the depths of 6–8 km affect the Platform units of Gran Sasso or the underlying units (e.g., Mot in Figure 5).

Velocity models interpretation reinforces the hypothesis that normal faults segmentation is due to intersection with NS trending thrust faults that often bisect older NW trending extensional systems. This is particularly evident for the southern termination of the PAGf, where the 2009 coseismic rupture abruptly terminates at the intersection with the Mot thrust (Figures 3 and 4) in correspondence of a more complex network of small fractures and faults (Valoroso et al., 2014). The limited lateral and vertical continuity of preexisting ramps, and the nonoptimal orientation within the mostly NE-SW oriented current extensional stress field (Mariucci & Montone, 2016), might result in a promotion of multiple mainshocks rather than large ruptures.

In this context, the identification of active faults from surface evidences is challenging. This ambiguity is exemplary for the MLGf segment, developed on the hanging wall of inherited compressive structures, where $M > 6.5$ earthquakes are hypothesized to occur (Galadini & Galli, 2003). The updip continuation of the deep ramp coincides with the surface fault expression that is still missing seismicity, both for 2009 and 2016–2018 seismic sequences. Seismicity that remained confined at depth greater than 5–6 km (Figure 6) might question the updip continuation of the fault.

We have explored different triggering mechanisms for the MLGf segment, including stress transfer (Stein, 1999; Toda et al., 2005) and pore fluid pressure migration (Chiarabba et al., 2009; Di Luccio et al., 2010; Malagnini et al., 2012; Miller et al., 2004). We modeled static stress changes on the fault, which were produced by all the large-magnitude earthquakes that occurred along the system since 2009 L'Aquila sequence (see the appendix for method). The stress increase reaches a maximum value of 0.8 MPa on the northern patches of the MLGf plane (Figure 7), while the southeastern portion of the ramp interested by the early 2017 seismicity was not significantly loaded. As a comparison, the stress variations accumulated before the occurrence of the October 2016 earthquakes shows increases up to 15 MPa (Figure 7). The evaluated ΔCFFs on the MLGf are 1 order of magnitude lower than the one computed on the October events fault

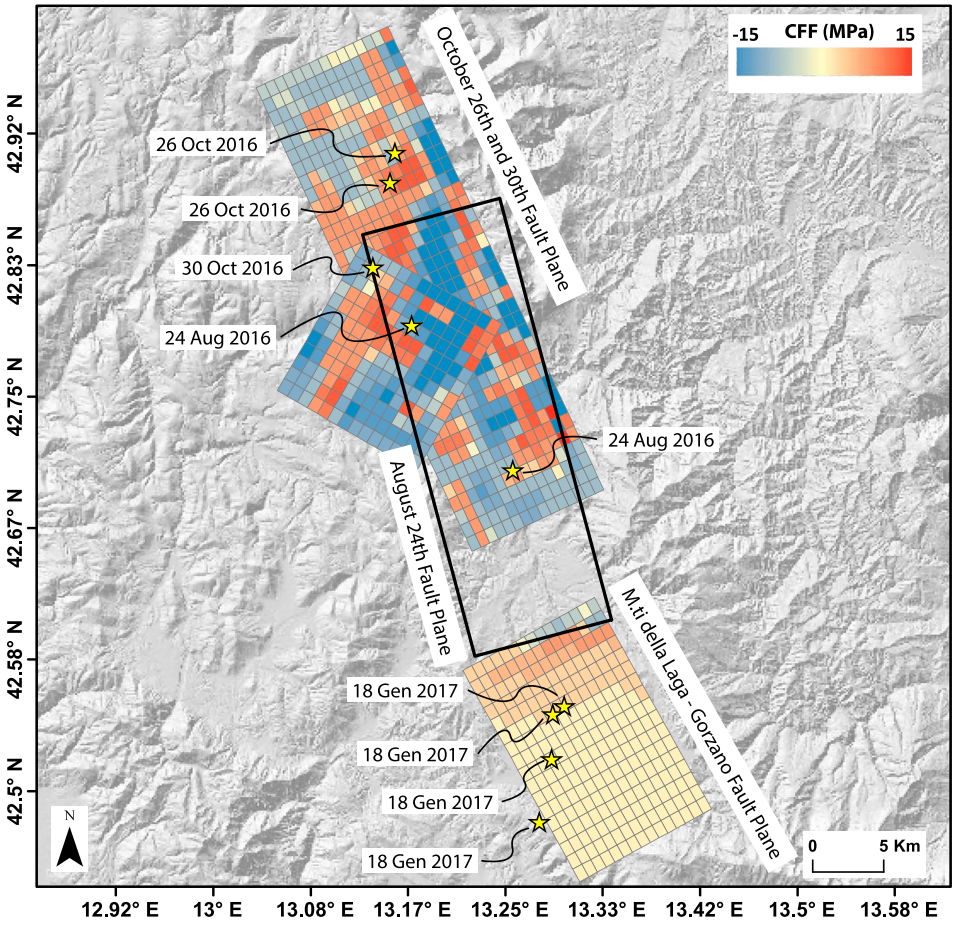

Figure 7. ΔCFF analysis results showing (1) the static stress changes calculated on the 2016 October fault planes due to the activation of the 24 August 2016 and October 2016 fault planes; (2) the stress changes on the Monti della laga-Gorzano fault plane due to 6 April 2009, the 24 August 2016, and the October 2016 earthquakes. CFF = Coulomb failure function.

planes. Effectively, the higher stress values are located in the northern portion of the fault, where, 65 days after the Amatrice earthquake, the 26 October Visso earthquake occurred. Anyway, the calculated value of 0.8 MPa is not negligible with respect to the minimum stress variation needed to generate seismicity on a critically stressed fault (0.01 MPa, e.g., Hardebeck et al., 1998).

In order to investigate fluid pressure trigger mechanism, we analyze the time change of V_P/V_s anomalies on the fault segment. We subdivided the entire period into two subepochs (Inversions labeled RealA and RealB, Figure 8), before and after the large shock occurred on the MLGf segment (the *Mw*5.6 shock on 9 April 2009). We used a total of 734 and 768 earthquakes for the two inversions, trying to achieve a similar spatial distribution and sampling as homogeneously as possible the target volume. This aspect is critical since hypocentral differences between earthquakes may result in projecting spatial difference of material properties into apparent temporal changes. Careful analysis of model resolution and synthetic tests confirm the reliability of time lapse imaging. Restore test indicates that the V_P/V_s anomalies are similarly reproduced, both in geometry and amplitude, for the two inversions (Figure 8). We obtained variance improvement of 53% and 60% and final root-mean-square of 0.11 and 010 s for RealA and RealB inversions, respectively.

Although the general trend of V_P/V_s anomalies in the two epochs is similar to that observed for the entire period (Figure 3), the prominent high V_P/V_s on the fault segment is visible only before the 9 April 2009 *Mw*5.6 earthquake (RealA in Figure 8). This anomaly sharply disappears after the large shock, reinforcing the hypothesis of fluid-triggering mechanism.

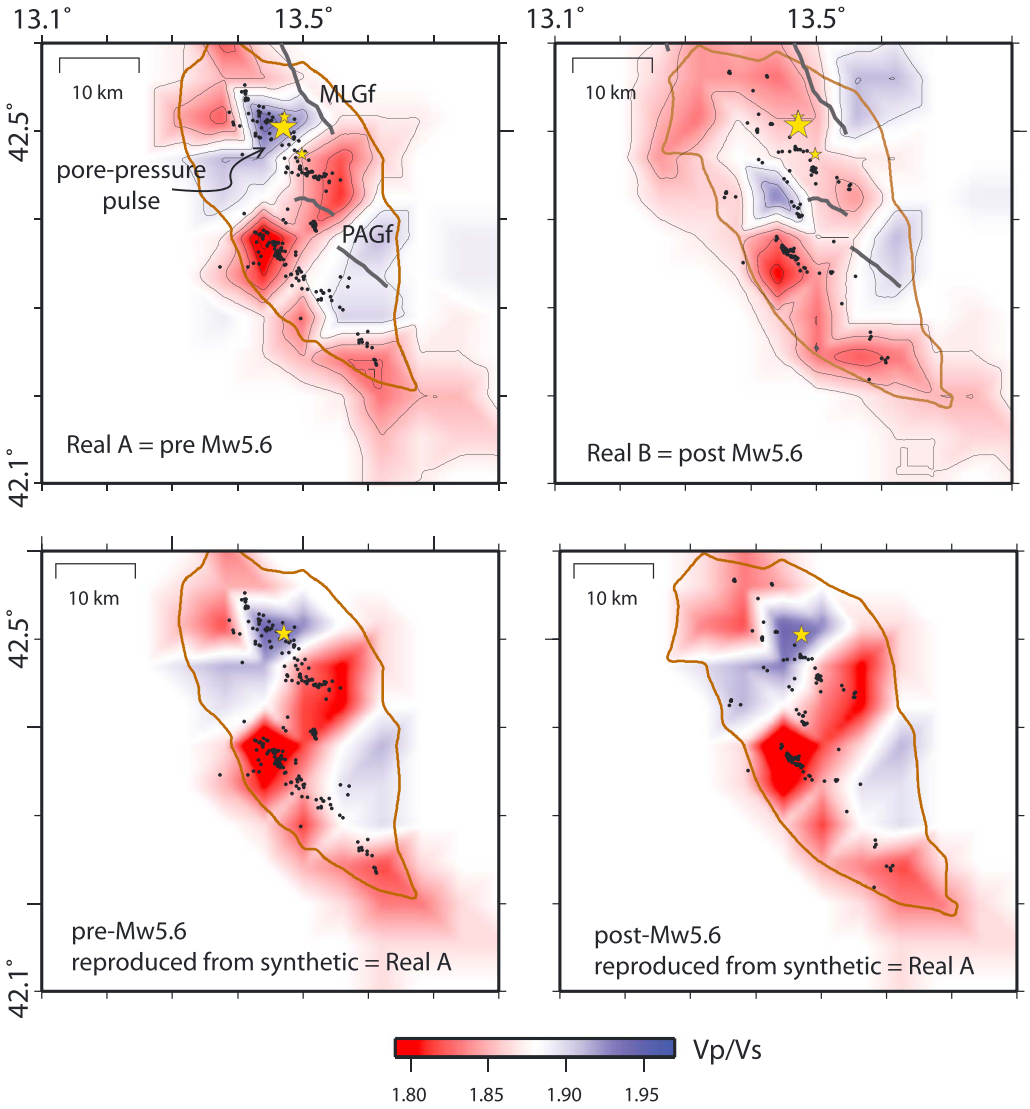

Figure 8. V_p/V_s models at 8-km depth computed before (RealA, top left panel) and after (RealB, top right panel) the large shock of April 2009 on the MLGf (yellow star). Earthquakes that occurred at those depths in the two periods are shown as black dots. Black lines are the surface traces of the MLGf and PAGf. Note the positive anomaly present on the segment before the event that vanishes in the period after. On the bottom panels, recovering of synthetic anomalies, which input is the model in RealA, for the two periods. Similar reproduction of features indicates similar resolution. MLGf = Monti della Laga-Gorzano fault; PAGf = Paganica fault.

No evident coseismic ruptures have been observed and no slip was modeled for the shallow portion of the MLGf, neither during the 2009 nor in the 2016–2017 sequences (Cheloni et al., 2017; Chiaraluce et al., 2017; Falcucci et al., 2016, 2009; Huang et al., 2017; Pucci et al., 2017). The maximum stress increase of about 0.8 MPa on the northern tip of the fault was then accumulated prevalently after the closest 24 August Amatrice earthquake (Figure 7). Assuming similar tectonic rates and an elapsed time since the last large earthquake on the MLGf not smaller than that on the Vettore fault system (at least in the last 1,500 years, see Galadini & Galli, 2003), a similar static stress increase (about 0.8 and 15 MPa, respectively) resulted in different potential triggering for the two faults. These evidences reinforce a more efficient Coulomb failure function (CFF) trigger mechanism on the Visso-Norcia fault planes with respect to the MLGf system.

On the other hand, we observe transient high V_p/V_s anomalies in the deeper part of the MLGf footwall (Figure 8) that we interpreted as overpressurized fluids. This might suggest a process similar to that observed during the 1997 Colfiorito (Chiarabba et al., 2009; Miller et al., 2004), the 2009 L'Aquila (Malagnini et al., 2012)

and the 2012 Emilia sequences (Pezzo et al., 2018), where the partial activation of the segment was interpreted as due to pore pressure diffusion. In this view, the transient pore pressure pulse for the 2009 large shock on the MLGf can be invoked as a viable triggering mechanism for multiple ruptures, as recently described by Walters et al. (2018) either for long clustered super seismic sequences (Chiarabba et al., 2011).

6. Conclusions

We investigate faulting mechanisms and interaction in a key area of the central Apennines where large earthquakes progressively propagated along a 150-km-long section of the normal faulting system. Fault segmentation during rupture evolution is mainly controlled by interference between inherited faults, derived from either the Mesozoic extension or the Miocene compression. We reveal a high V_p pristine Mesozoic structural high that conditioned the compressional tectonic phase with positive inversion of the bordering normal faults. Currently, deep normal faults and seismicity are rooted down to the base of these large and extremely high V_p bodies.

Since contiguous segments of the normal faulting system ruptured during past decades (i.e., the 2009 L'Aquila and 2016–2018 Amatrice earthquakes), the attention of scientific community started focusing on the unbroken segment of the MLGf. Our investigations suggest the lack of mechanical continuity between the deep ramp and the shallow expression of the fault, posing questions to the actual fault dimensions and the potential maximum magnitude still pending on such segment, after the several *M*5+ events occurred in past years. Since complexities and tectonic inversion are largely observed for collapsing fold and thrust belts like the Apennines, the revaluation of seismic hazard under the light of this results might represent a challenging issue for next decades.

Clustering of events might suggest the occurrence of an effective triggering mechanism among the segmented fault system. While we observe a significant CFF stress increase in the northern portion of the fault system ruptured by the 2016 October events, 1 order of magnitude lower values are found for the Monti della Laga-Gorzano fault. The different reaction of the entire system to static stress changes and the reconnaissance of transient high V_P/V_s anomalies associated to large aftershocks during the 2009 sequence led us to promote pore pressure pulses as a viable triggering mechanisms for the normal faulting earthquakes.

Appendix A

A1. Stress Transfer Method and Analysis

To analyze the impact of the recent closest large earthquakes on the Monti della laga-Gorzano fault, we perform a CFF analysis (e.g., Harris, 1998). Assuming no contribution of underground fluid pressure, the CFF can be defined as

CFF $= \tau + \mu'\sigma - S$,where τ is the shear stress projected on the target fault plane along the rake direction, σ is the stress normal to target fault plane, defined positive for traction, and μ is the apparent friction coefficient that takes into account the pressure effects. Over the timescales of our study, we consider the rock cohesion S as constant. Thus, considering the Coulomb stress variation, we can delete the unknown S and rewrite the ΔCFF as

$$\Delta\text{CFF} = \Delta\tau + \mu'\Delta\sigma,$$

where $\Delta\text{CFF} > 0$ could advance subsequent shocks toward failure and $\Delta\text{CFF} < 0$ values release stress and delay fault failure time. We fix the friction coefficient at 0.4, according to Harris (1998).

In this work, we evaluate the cumulated CFF variations along the MLGf plane due to the combined effects of the 6 April 2009 L'Aquila (*Mw* 6.1), the 24 August 2016 Amatrice (*Mw* 6.0), and the 26 October 2016 (*Mw* 5.9) and 30 October 2016 (*Mw* 6.5) earthquakes.

To evaluate the contribution of the Coulomb stress loading in the seismic sequence evolution, we also calculated the stress variations on the fault planes activated on 26 and 30 October Visso and Norcia earthquakes. Input seismic source parameters are from Atzori et al. (2009) and Scognamiglio et al. (2018) for L'Aquila and Visso-Norcia earthquakes, respectively. For the Amatrice events, we use the slip distribution obtained by Cheloni et al. (2017).

Acknowledgments

Authors would like to thank Luigi Improta for the stimulating discussions and suggestions during work activities and the two anonymous reviewers whose careful revisions sensibly improved the overall quality of the work. Data sets of the earthquakes location and tomographic inversion (Revelocity model of the study area) can be accessed at the following link: ftp://ftp.ingv.it/pub/mauro.buttinelli/TECT_018TC005053R/.

References

Atzori, S., Hunstad, I., Chini, M., Salvi, S., Tolomei, C., Bignami, C., et al. (2009). Finite fault inversion of DInSAR coseismic displacement of the 2009 L'Aquila earthquake (central Italy). *Geophysical Research Letters*, *36*, L15305. https://doi.org/10.1029/2009GL039293

Bally, A. W., Burbi, L., Cooper, C., & Ghelardoni, R. (1986). Balanced sections and seismic reflection profiles across the central Apennines. *Memorie Societá Geologica Italiana*, *35*(1), 257–310.

Barchi, M., Minelli, G., & Pialli, G. P. (1998). The CROP 03 profile: A synthesis of results on deep structures of the northern Apennines. *Memorie della Societa Geologica Italiana*, *52*, 383–400.

Bigi, S., Casero, P., Chiarabba, C., & Di Bucci, D. (2013). Contrasting surface active faults and deep seismogenic sources unveiled by the 2009 L'Aquila earthquake sequence (Italy). *Terra Nova*, *25*(1), 21–29. https://doi.org/10.1111/ter.12000

Bigi, S., Casero, P., & Ciotoli, G. (2011). Seismic interpretation of the Laga basin; constraints on the structural setting and kinematics of the central Apennines. *Journal of the Geological Society*, *168*(1), 179–190. https://doi.org/10.1144/0016-76492010-084

Boncio, P., Lavecchia, G., Milana, G., & Rozzi, B. (2004). Seismogenesis in central Apennines, Italy: An integrated analysis of minor earthquake sequences and structural data in the Amatrice-Campotosto area. *Annals of Geophysics*, *47*(6). https://doi.org/10.4401/ag-3371

Boncio, P., Lavecchia, G., & Pace, B. (2004). Defining a model of 3D seismogenic sources for seismic Hazard assessment applications: The case of central Apennines (Italy). *Journal of Seismology*, *8*(3), 407–425. https://doi.org/10.1023/B:JOSE.0000038449.78801.05

Bosi, C., Galadini, F., Giaccio, B., Messina, P., & Sposato, A. (2003). Plio-Quaternary continental deposits in the Latium-Abruzzi Apennines: the correlation of geological events across different intermontane basins. *Il Quaternario*, *16*(1Bis), 55–76.

Brace, W. F., & Kohlstedt, D. L. (1980). Limits on lithospheric stress imposed by laboratory experiments. *Journal of Geophysical Research*, *85*, 6248–6252. https://doi.org/10.1029/JB085iB11p06248

Butler, R. W. H., & Mazzoli, S. (2006). Styles of continental contraction: A review and introduction. In S. Mazzoli & R. W. H. Butler (Eds.), *Styles of continental contraction*, *Geol. Soc. Am., Special Paper* (Vol. 414, pp. 1–10). Boulder, CO. https://doi.org/10.1130/2006.2414(01)

Butler, R. W. H., Mazzoli, S., Corrado, S., De Donatis, M., Di Bucci, D., Gambini, R., et al. (2004). Applying thick-skinned tectonic models to the Apennine thrust belt of Italy: Limitations and implications. In K. R. McClay (Ed.), *Thrust tectonics and hydrocarbon systems*, *AAPG Memoirs* (Vol. 82, pp. 647–667). Boulder, Tulsa, OK.

Calabrò, R. A., Corrado, S., Di Bucci, D., Robustini, P., & Tornaghi, M. (2003). Thin-skinned vs. thick-skinned tectonics in the Matese massif, central–southern Apennines (Italy). *Tectonophysics*, *377*(3–4), 269–297. https://doi.org/10.1016/j.tecto.2003.09.010

Calamita, F., Paltrinieri, W., Pelorosso, M., Scisciani, V., & Tavarnelli, E. (2003). Inherited mesozoic architecture of the Adria continental paleomargin in the neogene central Apennines orogenic system, Italy. *Boll Soc Geol It*, *122*, 307–318.

Carannante, S., Monachesi, G., Cattaneo, M., Amato, A., & Chiarabba, C. (2013). Deep structure and tectonics of the northern-central Apennines as seen by regional-scale tomography and 3-D located earthquakes. *Journal of Geophysical Research: Solid Earth*, *118*, 5391–5403. https://doi.org/10.1002/jgrb.50371

Cardello, G. L., & Doglioni, C. (2015). From mesozoic rifting to Apennine orogeny: The Gran Sasso range (Italy). *Gondwana Research*, *27*(4), 1307–1334. https://doi.org/10.1016/j.gr.2014.09.009

Castellarin, A., Colacicchi, R., & Praturlon, A. (1978). Fasi distensive, trascorrenze e sovrascorrimenti lungo la" Linea Ancona-Anzio", dal Lias medio al Pliocene. Pinto.

Centamore E., Adamoli L., Berti D., Bigi S., Casnedi R., Cantalamessa G., et al. (1992). Carta geologica dei bacini della Laga e del Cellino e dei rilievi carbonatici circostanti (Marche meridionali, Lazio nord-orientale, Abruzzo settentrionale). Scala 1:100.000. S.EL.C.A., Firenze.

Centamore, E., Cantalamessa, G., Micarelli, A., Potetti, M., Ridolfi, M., Cristallini, C., & Morelli, C. (1993). Contributo alla conoscenza dei depositi terrigeni neogenici di avanfossa del teramano (Abruzzo settentrionale). *Bollettino della Societa Geologica Italiana*, *112*(1), 63–81.

Cheloni, D., De Novellis, V., Albano, M., Antonioli, A., Anzidei, M., Atzori, S., et al. (2017). Geodetic model of the 2016 Central Italy earthquake sequence inferred from InSAR and GPS data. *Geophysical Research Letters*, *44*, 6778–6787. https://doi.org/10.1002/2017GL073580

Chiarabba, C., & Amato, A. (2003). Vp and Vp/Vs images in the *Mw* 6.0 Colfiorito fault region (central Italy): A contribution to the understanding of seismotectonic and seismogenic processes. *Journal of Geophysical Research*, *108*(B5), 2248. https://doi.org/10.1029/2001JB001665

Chiarabba, C., Amato, A., Anselmi, M., Baccheschi, P., Bianchi, I., Cattaneo, M., et al. (2009). The 2009 L'Aquila (Central Italy) *Mw*6. 3 earthquake: Main shock and aftershocks. *Geophysical Research Letters*, *36*, L18308. https://doi.org/10.1029/2009GL039627

Chiarabba, C., & Chiodini, G. (2013). Continental delamination and mantle dynamics drive topography, extension and fluid discharge in the Apennines. *Geology*, *41*(6), 715–718. https://doi.org/10.1130/G33992.1

Chiarabba, C., De Gori, P., & Amato, A. (2011). Do earthquake storms repeat in the Apennines of Italy? *Terra Nova*, *23*(5), 300–306. https://doi.org/10.1111/j.1365-3121.2011.01013.x

Chiarabba, C., De Gori, P., & Mele, F. M. (2015). Recent seismicity of Italy: Active tectonics of the central Mediterranean region and seismicity rate changes after the Mw 6.3 L'Aquila earthquake. *Tectonophysics*, *638*, 82–93.

Chiarabba, C., Jovane, L., & DiStefano, R. (2005). A new view of Italian seismicity using 20 years of instrumental recordings. *Tectonophysics*, *395*(3–4), 251–268. https://doi.org/10.1016/j.tecto.2004.09.013

Chiaraluce, L., Di Stefano, R., Tinti, E., Scognamiglio, L., Michele, M., Casarotti, E., et al. (2017). The 2016 Central Italy seismic sequence: A first look at the mainshocks, aftershocks, and source models. *Seismological Research Letters*, *88*(3), 757–771. https://doi.org/10.1785/0220160221

Chiaraluce, L., Valoroso, L., Piccinini, D., Di Stefano, R., & De Gori, P. (2011). The anatomy of the 2009 L'Aquila normal fault system (central Italy) imaged by high resolution foreshock and aftershock locations. *Journal of Geophysical Research*, *116*, B12311. https://doi.org/10.1029/2011JB008352

Cirella, A., Piatanesi, A., Tinti, E., Chini, M., & Cocco, M. (2012). Complexity of the rupture process during the 2009 L'Aquila, Italy, earthquake. *Geophysical Journal International*, *190*(1), 607–621. https://doi.org/10.1111/j.1365-246X.2012.05505.x

Cloetingh, S., & Burov, E. B. (1996). Thermomechanical structure of European continental lithosphere: Constraints from rheological profiles and EET estimates. *Geophysical Journal International*, *124*(3), 695–723. https://doi.org/10.1111/j.1365-246X.1996.tb05633.x

Coward, M. P. (1994). Continental collision. In P. L. Hancock (Ed.), *Inversion tectonics* (pp. 289–304). New York: Pergamon Press.

Cowie, P. A., Roberts, G. P., Bull, J. M., & Visini, F. (2012). Relationships between fault geometry, slip rate variability and earthquake recurrence in extensional settings. *Geophysical Journal International*, *189*(1), 143–160. https://doi.org/10.1111/j.1365-246X.2012.05378.x

D'Agostino, N., Mantenuto, S., D'Anastasio, E., Avallone, A., Barchi, M., Collettini, C., et al. (2009). Contemporary crustal extension in the Umbria–Marche Apennines from regional CGPS networks and comparison between geodetic and seismic deformation. *Tectonophysics*, *476*(1–2), 3–12. https://doi.org/10.1016/j.tecto.2008.09.033

Di Domenica, A., Turtù, A., Satolli, S., & Calamita, F. (2012). Relationships between thrusts and normal faults in curved belts: New insight in the inversion tectonics of the central-northern Apennines (Italy). *Journal of Structural Geology*, *42*, 104–117. https://doi.org/10.1016/j.jsg.2012.06.008

Di Luccio, F., Ventura, G., Di Giovambattista, R., Piscini, A., & Cinti, F. R. (2010). Normal faults and thrusts reactivated by deep fluids: The 6 April 2009 *Mw* 6.3 L'Aquila earthquake, central Italy. *Journal of Geophysical Research*, *115*, B06315. https://doi.org/10.1029/2009JB007190

Di Stefano, R., Chiarabba, C., Chiaraluce, L., Cocco, M., De Gori, P., Piccinini, D., & Valoroso, L. (2011). Fault zone properties affecting the rupture evolution of the 2009 (*Mw* 6.1) L'Aquila earthquake (central Italy): Insights from seismic tomography. *Geophysical Research Letters*, *38*, L10310. https://doi.org/10.1029/2011GL047365

Doglioni, C. (1991). A proposal for the kinematic modelling of W-dipping subductions-possible applications to the Tyrrhenian-Apennines system. *Terra Nova*, *3*(4), 423–434. https://doi.org/10.1111/j.1365-3121.1991.tb00172.x

Eberhart-Phillips, D., & Reyners, M. (1997). Continental subduction and three-dimensional crustal structure: The northern South Island, New Zealand. *Journal of Geophysical Research*, *102*, 11,843–11,861. https://doi.org/10.1029/96JB03555

Falcucci, E., Gori, S., Bignami, C., Pietrantonio, G., Melini, D., Moro, M., et al. (2018). The Campotosto Seismic Gap in Between the 2009 and 2016–2017 Seismic Sequences of Central Italy and the Role of Inherited Lithospheric Faults in Regional Seismotectonic Settings. *Tectonics*, *37*, 2425–2445. https://doi.org/10.1029/2017TC004844

Falcucci, E., Gori, S., Galadini, F., Fubelli, G., Moro, M., & Saroli, M. (2016). Active faults in the epicentral and mesoseismal M_L 6.0 24, 2016 Amatrice earthquake region, central Italy. Methodological and seismotectonic issues. *Annals of Geophysics*, *59*. https://doi.org/10.4401/ag-7266

Falcucci, E., Gori, S., Peronace, E., Fubelli, G., Moro, M., Saroli, M., et al. (2009). The Paganica fault and surface coseismic ruptures caused by the 6 April 2009 earthquake (L'Aquila, central Italy). *Seismological Research Letters*, *80*(6), 940–950. https://doi.org/10.1785/gssrl.80.6.940

Fletcher, J. M., Oskin, M. E., & Teran, O. J. (2016). The role of a keystone fault in triggering the complex El Mayor–Cucapah earthquake rupture. *Nature Geoscience*, *9*(4), 303–307. https://doi.org/10.1038/ngeo2660

Freed, A. M. (2005). Earthquake triggering by static, dynamic, and postseismic stress transfer. *Annual Review of Earth and Planetary Sciences*, *33*(1), 335–367. https://doi.org/10.1146/annurev.earth.33.092203.122505

Galadini, F., & Galli, P. (2003). Paleoseismology of silent faults in the central Apennines (Italy): The Mt. Vettore and Laga Mts. Faults. *Annals of Geophysics*. https://doi.org/10.4401/ag-3457

Hamling, I. J., Hreinsdóttir, S., Clark, K., Elliott, J., Liang, C., Fielding, E., et al. (2017). Complex multifault rupture during the 2016 *Mw* 7.8 Kaikōura earthquake, New Zealand. *Science*, *356*(6334), eaam7194. https://doi.org/10.1126/science.aam7194

Hardebeck, J. L., Nazareth, J. J., & Hauksson, E. (1998). The static stress change triggering model: Constraints from two southern California aftershocks. *Journal of Geophysical Research*, *103*, 24,427–24,437. https://doi.org/10.1029/98JB00573

Harris, R. A. (1998). Introduction to special section: Stress triggers, stress shadows, and implications for seismic hazard. *Journal of Geophysical Research*, *103*, 24,347–24,358. https://doi.org/10.1029/98JB01576

Huang, M.-H., Fielding, E. J., Liang, C., Milillo, P., Bekaert, D., Dreger, D., & Salzer, J. (2017). Coseismic deformation and triggered landslides of the *Mw* 6.2 Amatrice earthquake in Italy. *Geophysical Research Letters*, *44*, 1266–1274. https://doi.org/10.1002/2016GL071687

Improta, L., Villani, F., Bruno, P. P., Castiello, A., De Rosa, D., Varriale, F., et al. (2012). High-resolution controlled-source seismic tomography across the Middle Aterno basin in the epicentral area of the 2009, *Mw* 6.3, L'Aquila earthquake (central Apennines, Italy). *Italian Journal of Geosciences*, *131*(3), 373–388. https://doi.org/10.3301/IJG.2011.35

Jackson, J. (1995). Continental deformation. In P. L. Hancock, (ed.) 1994. xi 421 pp. Oxford, New York, Seoul, Tokyo: Pergamon Press. ISBN 0 08 037931 1; 0 08 037930 3 (pb). *Geological Magazine*, *132*(1), 130–130. https://doi.org/10.1017/S0016756800011602

Jackson, J. A. (1980). Reactivation of basement faults and crustal shortening in orogenic belts. *Nature*, *283*(5745), 343–346. https://doi.org/10.1038/283343a0

Latorre, D., Mirabella, F., Chiaraluce, L., Trippetta, F., & Lomax, A. (2016). Assessment of earthquake locations in 3-D deterministic velocity models: A case study from the Altotiberina Near Fault Observatory (Italy). *Journal of Geophysical Research: Solid Earth*, *121*, 8113–8135. https://doi.org/10.1002/2016JB013170

Lavecchia, G., Castaldo, R., De Nardis, R., De Novellis, V., Ferrarini, F., Pepe, S., et al. (2016). Ground deformation and source geometry of the 24 August 2016 Amatrice earthquake (Central Italy) investigated through analytical and numerical modeling of DInSAR measurements and structural-geological data. *Geophysical Research Letters*, *43*, 12,389–12,398. https://doi.org/10.1002/2016GL071723

Malagnini, L., Lucente, F. P., De Gori, P., Akinci, A., & Munafo, I. (2012). Control of pore fluid pressure diffusion on fault failure mode: Insights from the 2009 L'Aquila seismic sequence. *Journal of Geophysical Research*, *117*, B05302. https://doi.org/10.1029/2011JB008911

Margheriti, L., Chiaraluce, L., Voisin, C., Cultrera, G., Govoni, A., Moretti, M., et al. (2011). Rapid response seismic networks in Europe: Lessons learnt from the L'Aquila earthquake emergency. *Annals of Geophysics*, *54*(4), 392–399. https://doi.org/10.4401/ag-4953

Mariucci, M. T., & Montone, P. (2016). Contemporary stress field in the area of the 2016 Amatrice seismic sequence (central Italy). *Annals of Geophysics*, *59*. https://doi.org/10.4401/ag-7235

Martínez-Garzón, P., Bohnhoff, M., Ben-Zion, Y., & Dresen, G. (2015). Scaling of maximum observed magnitudes with geometrical and stress properties of strike-slip faults. *Geophysical Research Letters*, *42*, 10,230–10,238. https://doi.org/10.1002/2015GL066478

Mazzoli, S., Cello, G., Deiana, G., Galdenzi, S., Gambini, R., Mancinelli, A., et al. (2000). Modes of foreland deformation ahead of the Apennine thrust front. *Journal of the Czech Geological Society*, *45*, 246.

Miller, S. A., Collettini, C., Chiaraluce, L., Cocco, M., Barchi, M., & Kaus, B. J. (2004). Aftershocks driven by a high-pressure CO_2 source at depth. *Nature*, *427*(6976), 724–727. https://doi.org/10.1038/nature02251

Palumbo, L., Benedetti, L., Bourles, D., Cinque, A., & Finkel, R. (2004). Slip history of the Magnola fault (Apennines, Central Italy) from 36Cl surface exposure dating: Evidence for strong earthquakes over the Holocene. *Earth and Planetary Science Letters*, *225*(1–2), 163–176. https://doi.org/10.1016/j.epsl.2004.06.012

Patacca, E., Sartori, R., & Scandone, P. (1990). Tyrrhenian basin and Apenninic arcs: Kinematic relations since Late Tortonian times. *Memorie della Societa Geologica Italiana*, *45*, 425–451.

Pezzo, G., De Gori, P., Lucente, F. P., & Chiarabba, C. (2018). Pore pressure pulse drove the 2012 Emilia (Italy) series of earthquakes. *Geophysical Research Letters*, *45*, 682–690. https://doi.org/10.1002/2017GL076110

Pfiffner, O. A. (2017). Thick-skinned and thin-skinned tectonics: A global perspective. *Geosciences*, *7*(3), 71. https://doi.org/10.3390/geosciences7030071

Pizzi, A., Di Domenica, A., Gallovič, F., Luzi, L., & Puglia, R. (2017). Fault segmentation as constraint to the occurrence of the main shocks of the 2016 central Italy seismic sequence. *Tectonics*, *36*, 2370–2387. https://doi.org/10.1002/2017TC004652

Porreca, M., Minelli, G., Ercoli, M., Brobia, A., Mancinelli, P., Cruciani, F., et al. (2018). Seismic reflection profiles and subsurface geology of the area interested by the 2016–2017 earthquake sequence (Central Italy). *Tectonics*, *37*, 1116–1137. https://doi.org/10.1002/2017TC004915

Pucci, S., De Martini, P. M., Civico, R., Villani, F., Nappi, R., Ricci, T., et al. (2017). Coseismic ruptures of the 24 August 2016, *Mw* 6.0 Amatrice earthquake (central Italy). *Geophysical Research Letters*, *44*, 2138–2147. https://doi.org/10.1002/2016GL071859

Pucci, S., Mirabella, F., Pazzaglia, F., Barchi, M. R., Melelli, L., Tuccimei, P., et al. (2014). Interaction between regional and local tectonic forcing along a complex Quaternary extensional basin: Upper Tiber Valley, Northern Apennines, Italy. *Quaternary Science Reviews*, *102*, 111–132.

Ranalli, G., & Murphy, D. C. (1987). Rheological stratification of the lithosphere. *Tectonophysics*, *132*(4), 281–295. https://doi.org/10.1016/0040-1951(87)90348-9

Rovida, A., Camassi, R., Gasperini, P., & Stucchi, M. (2011). Catalogo Parametrico dei Terremoti Italiani.

Scisciani, V. (2009). Styles of positive inversion tectonics in the central Apennines and in the Adriatic foreland: Implications for the evolution of the Apennine chain (Italy). *Journal of Structural Geology*, *31*(11), 1276–1294. https://doi.org/10.1016/j.jsg.2009.02.004

Scisciani, V., Agostini, S., Calamita, F., Pace, P., Cilli, A., Giori, I., & Paltrinieri, W. (2014). Positive inversion tectonics in foreland fold-and-thrust belts: A reappraisal of the Umbria–Marche northern Apennines (central Italy) by integrating geological and geophysical data. *Tectonophysics*, *637*, 218–237. https://doi.org/10.1016/j.tecto.2014.10.010

Scisciani, V., & Montefalcone, R. (2005). Evoluzione neogenico-quaternaria del fronte della catena centro-appenninica; vincoli dal bilanciamento sequenziale di una sezione geologica regionale. *Bollettino della Società Geologica Italiana*, *124*(3), 579–599.

Scognamiglio, L., Tinti, E., Casarotti, E., Pucci, S., Villani, F., Cocco, M., Magnoni, F., et al. (2018). Complex fault geometry and rupture dynamics of the *Mw* 6.5, 30 October 2016, Central Italy earthquake. *Journal of Geophysical Research: Solid Earth*, *123*, 2943–2964. https://doi.org/10.1002/2018JB015603

Scrocca, D., Carminati, E., & Doglioni, C. (2005). Deep structure of the southern Apennines, Italy: Thin-skinned or thick-skinned? *Tectonics*, *24*, TC3005. https://doi.org/10.1029/2004TC001634

Scrocca, D., Carminati, E., Doglioni, C., & Marcantoni, D. (2007). Slab retreat and active shortening along the central-northern Apennines. In *Thrust belts and foreland basins* (pp. 471–487). Berlin, Heidelberg: Springer. https://doi.org/10.1007/978-3-540-69426-7_25

Scrocca, D., Doglioni, C., & Innocenti, F. (2003). Constraints for an interpretation of the Italian geodynamics: A review. *Memorie Descrittive della Carta Geologica d'Italia*, *62*, 15–46.

Serpelloni, E., Anzidei, M., Baldi, P., Casula, G., & Galvani, A. (2005). Crustal velocity and strain-rate fields in Italy and surrounding regions: New results from the analysis of permanent and non-permanent GPS networks. *Geophysical Journal International*, *161*(3), 861–880. https://doi.org/10.1111/j.1365-246X.2005.02618.x

Shiner, P., Beccacini, A., & Mazzoli, S. (2004). Thin-skinned versus thick-skinned structural models for Apulian carbonate reservoirs: Constraints from the Val d'Agri Fields, S Apennines, Italy. *Marine and Petroleum Geology*, *21*(7), 805–827. https://doi.org/10.1016/j.marpetgeo.2003.11.020

Sieh, K., Jones, L., Hauksson, E., Hudnut, K., Eberhart-Phillips, D., Heaton, T., et al. (1993). Near-field investigations of the Landers earthquake sequence, April to July 1992. *Science*, *260*(5105), 171–176. https://doi.org/10.1126/science.260.5105.171

Stein, R. S. (1999). The role of stress transfer in earthquake occurrence. *Nature*, *402*(6762), 605–609. https://doi.org/10.1038/45144

Tinti, E., Scognamiglio, L., Michelini, A., & Cocco, M. (2016). Slip heterogeneity and directivity of the M_L 6.0, 2016, Amatrice earthquake estimated with rapid finite-fault inversion. *Geophysical Research Letters*, *43*, 10,745–10,752. https://doi.org/10.1002/2016GL071263

Toda, S., Stein, R. S., Richards-Dinger, K., & Bozkurt, S. B. (2005). Forecasting the evolution of seismicity in southern California: Animations built on earthquake stress transfer. *Journal of Geophysical Research*, *110*, B05S16. https://doi.org/10.1029/2004JB003415

Toomey, D. R., & Foulger, G. R. (1989). Tomographic inversion of local earthquake data from the Hengill-Grensdalur central volcano complex, Iceland. *Journal of Geophysical Research*, *94*, 17,497–17,510. https://doi.org/10.1029/JB094iB12p17497

Tozer, R. S. J., Butler, R. W. H., & Corrado, S. (2002). Comparing thin-and thick-skinned thrust tectonic models of the central Apennines, Italy. *EGU Stephan Mueller Special Publication Series*, *1*, 181–194.

Valoroso, L., Chiaraluce, L., & Collettini, C. (2014). Earthquakes and fault zone structure. *Geology*, *42*(4), 343–346. https://doi.org/10.1130/G35071.1

Valoroso, L., Chiaraluce, L., Piccinini, D., Di Stefano, R., Schaff, D., & Waldhauser, F. (2013). Radiography of a normal fault system by 64,000 high-precision earthquake locations: The 2009 L'Aquila (central Italy) case study. *Journal of Geophysical Research: Solid Earth*, *118*, 1156–1176. https://doi.org/10.1002/jgrb.50130

Walters, R. J., Gregory, L. C., Wedmore, L. N. J., Craig, T. J., McCaffrey, K., Wilkinson, M., Chen, J., et al. (2018). Dual control of fault intersections on stop-start rupture in the 2016 Central Italy seismic sequence. *Earth and Planetary Science Letters*, *500*, 1–14. https://doi.org/10.1016/j.epsl.2018.07.043

Ziegler, P. A., Cloetingh, S., & van Wees, J. D. (1995). Dynamics of intra-plate compressional deformation: The Alpine foreland and other examples. *Tectonophysics*, *252*(1–4), 7–59. https://doi.org/10.1016/0040-1951(95)00102-6